

## Cellular Targets of Infection and Route of Viral Dissemination after an Intravaginal Inoculation of Simian Immunodeficiency Virus into Rhesus Macaques

By Alexander I. Spira,\* Preston A. Marx,\* Bruce K. Patterson,†§ James Mahoney,|| Richard A. Koup,\* Steven M. Wolinsky,‡ and David D. Ho\*

From the \*Aaron Diamond AIDS Research Center, New York University School of Medicine, New York 10016; the †Department of Medicine and the ‡Department of Pathology, Northwestern University Medical School, Chicago, Illinois 60611; and the §Laboratory for Experimental Medicine and Surgery in Primates, New York University Medical Center, Tuxedo, New York 10957

### Summary

We used the simian immunodeficiency virus (SIV)/rhesus macaque model to study events that underlie sexual transmission of human immunodeficiency virus type 1 (HIV-1). Four female rhesus macaques were inoculated intravaginally with SIVmac251, and then killed 2, 5, 7, and 9 d later. A technique that detected polymerase chain reaction–amplified SIV *in situ* showed that the first cellular targets for SIV were in the lamina propria of the cervicovaginal mucosa, immediately subjacent to the epithelium. Phenotypic and localization studies demonstrated that many of the infected cells were likely to be dendritic cells. Within 2 d of inoculation, infected cells were identified in the paracortex and subcapsular sinus of the draining internal iliac lymph nodes. Subsequently, systemic dissemination of SIV was rapid, since culturable virus was detectable in the blood by day 5. From these results, we present a model for mucosal transmission of SIV and HIV-1.

**E**pidemic spread of human HIV-1 occurs primarily as the result of sexual transmission from infected individuals, via free virions or cell-associated virus present in the genital secretions. Although the greatest likelihood of HIV-1 spread is from an infected male during anal or vaginal intercourse, the process is still not efficient. It is estimated that from an HIV-1–infected male, sexual transmission to a female with a single contact carries an infectivity rate of 0.3% (1). In comparison, one such sexual exposure to a hepatitis B–infected individual carries an infectivity rate of 20–30% (2). Defining the mechanism of sexual transmission, namely, how HIV-1 trafficks across the mucosal surface and spreads to distal sites, is important not only for understanding the pathogenesis of HIV-1 infection, but also for the development of a protective vaccine.

Characterization of the virus present in acute HIV-1 seroconvertors has yielded information about the types of viruses that are found after sexual transmission. In a newly infected individual, the HIV-1 quasispecies appear to be extremely homogeneous, even when the transmitter of that virus has a diverse mixture of genotypes (3). These studies also demonstrated that the transmitted virus often represents only a minor variant of those viruses present in the blood of the transmitter; similar findings have been seen in

maternal–fetal transmission of HIV-1 (4). Although still a minor species, the transmitted variant is usually present in higher amounts in the seminal cells and seminal plasma than in the PBMC and plasma of the transmitters (4a). During sexual transmission, there is also a selection for viral phenotype. Even when a transmitter harbors a mixture of viral phenotypes, the newly infected person usually has a nonsyncytium-inducing virus that is macrophage tropic (3, 5), although exceptions to this have been noted (6). Sequence analysis of transmitted variants has demonstrated a higher selective pressure on the viral envelope protein, gp120, which governs many aspects of the viral phenotype (3, 7–9). These findings point to a bottleneck that selects for particular viral variants during sexual transmission. A possible location for such a bottleneck is the mucosal surface, which poses a formidable barrier to HIV-1 transmission (2, 3).

It is crucial to understand how HIV-1 disseminates from an initial site of infection to generate a large burst of viremia during primary infection. The initial viremia is subsequently reduced by several orders of magnitude (10, 11), a phenomenon that correlates with the appearance of cell-mediated immunity (12). In spite of this efficient control, most individuals remain detectably viremic, and the con-

tinuous high-level viral production eventually leads to immunosuppression and AIDS (13, 14). Although numerous hypotheses on the mechanisms of transmission have been proposed based on studies of chronically infected humans (15–17) or macaques (18–20), to date none has looked directly at acutely infected subjects to identify the initial cellular target and pathway of virus dissemination after exposure of an intact mucosal epithelium to virus.

For these reasons, we aimed to study the earliest events that follow an intravaginal transmission of virus. To do this in HIV-1-infected humans is nearly impossible, since infected patients generally do not present until they are symptomatic, when viral dissemination has already occurred. Thus, we used the simian immunodeficiency virus (SIV)<sup>1</sup>/rhesus macaque system, the animal model that most closely resembles HIV-1 infection in humans (21). In many ways, SIV and HIV-1 are very similar, as are the disease courses they induce (22, 23). Using cell-free SIVmac251 and female rhesus macaques, a model of atraumatic vaginal transmission has been established (18). We infected four female macaques in this manner, followed by serial killings 2–9 d later. Using *in situ* PCR to amplify SIV DNA for subsequent detection and immunocytochemistry, we determined the location and phenotype of the first cellular targets of infection in the cervicovaginal mucosa. We also characterized the route and time course of viral spread from the genital mucosa to the proximal draining lymph nodes, then to the distal lymphatic tissues. Based on these studies, we present a model of mucosal transmission and dissemination of SIV that has relevance to the sexual transmission of HIV-1.

## Materials and Methods

**Animals.** All animals used in this study were multiparous adult female rhesus macaques (*Macaca mulatta*) at the Laboratory for Experimental Medicine and Surgery in Primates (Tuxedo, NY). Before use, the animals were negative for antibodies to HIV-2, SIV, type D retrovirus, and simian T cell leukemia virus, type I. This study protocol was reviewed and approved by the institutional animal care and use committee.

**Inoculations.** The virus stock used for this study was SIVmac251 (23). This cell-free inoculum was grown in human PBMC (18) from a stock obtained from R. C. Desrosiers of the New England Regional Primate Research Center (Southborough, MA) and contained  $10^3$  TCID<sub>50</sub> (50% tissue culture infectious doses per milliliter) (24). Inocula were cryopreserved, and then thawed at 37°C immediately before use.

The animals were immobilized with an intramuscular injection of ketamine HCl (10 mg/kg). A human nasal speculum was then inserted into the vaginal canal, followed by a pediatric nasogastric feeding tube (2.5 mm outer diameter, 8 french). 1 ml of the inoculum was then infused with a syringe through the tube over a course of ~5 min. After removal of the tube, the vaginal canal was then visually inspected to ensure no trauma was induced by the procedure.

After removal of the speculum, the monkeys were vertically inverted and remained immobilized until the anesthetic wore off in ~45 min to 1 h. The inoculum remained inside the vaginal canal until it was absorbed.

Control animals consisted of an uninfected monkey that was killed because of amyloidosis of the liver (Rh Co) and an animal that was inoculated with the same viral stock that had been heat inactivated at 56°C for 2.5 h (Rh HI). Inactivation was verified by culturing 10 µl of the inoculum before and after heating (see below).

**Necropsy and Tissue Processing.** One animal was killed at each time point, 2, 5, 7, and 9 d after inoculation. Animals killed at the later time points were bled at the earlier time points (10 ml whole blood; see Table 1), and plasma and PBMC were obtained as described below. Before necropsy, the animals were again immobilized with ketamine. Peripheral lymph nodes were obtained bilaterally from the axillary and inguinal regions. A vertical abdominal incision was made, and the internal iliac and common iliac lymph nodes were removed by dissection along the internal and common iliac blood vessels. A terminal bleed was then performed through the abdominal aorta, along with an intravenous overdose of phenobarbital. Finally, the spleen, vagina, cervix, and uterus were removed.

PBMC from heparinized whole blood and splenic lymphocytes were isolated by Ficoll-Hypaque (Organon Teknika, Durham, NC) gradient centrifugation as previously described (25). Lymph nodes were dissected, and lymph node mononuclear cells (LNMC) were isolated in PBS. The remainder of the nodes and spleen, vagina, cervix, and uterus were cut into pieces of ~0.5 × 1 cm, washed in PBS, and put into Streck's tissue fixative (STF; Streck Laboratories, Inc., Omaha, NE) for 1 wk. The tissues were then embedded into paraffin using an automated tissue processor, under heat and vacuum pressure. Tissues from control and test animals were processed in an identical manner.

**Virus Isolation.** From the terminal bleeds,  $2 \times 10^7$  PBMC and  $2\text{--}5 \times 10^7$  LNMC were added to  $5 \times 10^6$  CEMx174 cells (26) in 20 ml of RPMI 1640 media supplemented with 10% heat-inactivated FCS, penicillin (250 U/ml), streptomycin (250 µg/ml), and 10 mM Hepes. 1 ml plasma and  $2 \times 10^6$  PBMC from preterminal time points were cocultured in 1.5 ml supplemented media with  $2 \times 10^6$  CEMx174 cells. After 1 wk, half the cells and media were removed and fresh media were added twice each week for 8 wk. The cultures were monitored for cytopathic effects (syncytium formation) and assayed using an immunoassay for SIV gp120 production as previously described (27). Briefly, culture supernatants (1:3) were added to a solid phase containing the sheep polyclonal antibody D7369 (Aalto BioReagents, Dublin, Ireland), and bound gp120 was detected using serum from an SIV-infected macaque, followed by alkaline phosphatase-conjugated anti-human IgG (Accurate Chemicals, Westbury, NY) and the AMPAK detection system (Dako Diagnostics, Carpinteria, CA). All positive cultures had optical densities at 492 nm >1.00 at all time points after the third week of culture. All negative cultures had optical densities <0.075, which were equivalent to background levels in the assay. Using purified SIVmac239 gp140, SIVmac1A11 gp140, and SIVmac239 gp130 obtained through the AIDS Research and Reference Reagent Program, National Institute of Allergy and Infectious Diseases (NIAID), National Institutes of Health (NIH, Bethesda, MD), this assay was determined to be sensitive to <25 pg of gp120/ml of supernatant.

**PCR and In Situ PCR.** Genomic DNA was isolated from STF-fixed, paraffin-embedded blocks as follows. Between 6 and 10 8-µm sections were cut with a clean, disposable microtome blade

<sup>1</sup>Abbreviations used in this paper: BCIP, 5-bromo-4-chloro-3-indolyl phosphate; LNMC, lymph node mononuclear cells; NBT, nitroblue tetrazolium; SIV, simian immunodeficiency virus; STF, Streck's tissue fixative.

from each block and placed into a sterile Eppendorf tube. The samples were deparaffinized twice with 1 ml xylene for 30 min at room temperature, and the xylene was removed with two 15-min washes of 100% ethanol. After drying the tissue in a 60°C oven for 30 min, the samples were digested in 300  $\mu$ l of lysis buffer (50 mM Tris, pH 8.0, 1 mM EDTA, 0.5% Tween 20) containing 200  $\mu$ g/ml proteinase K for 2 h at 55°C. The samples were extracted two to three times with 1:1 phenol/chloroform and then two to three times with chloroform. Genomic DNA was precipitated in ethanol overnight at -40°C, washed in 70% ethanol, dried, and resuspended in water. Genomic DNA was isolated from PBMC by extraction with a guanidinium isothiocyanate-based DNA extraction kit (United States Biochemical Corp., Cleveland, OH), following the manufacturer's instructions.

From 0.2 to 2  $\mu$ g of the genomic DNA in a volume of 5  $\mu$ l were then used in a nested PCR for SIV gag. Outer primers were AS29 (+): 5'-CGTCTTGTCAGGGAAGAAAGCAGATGAAT-3' (corresponding to bases 1058-1087 of the SIVmac251 genome), and AS30 (-): 5'-CTTCCTCAGTGTGTTTCACTTCTCTT-3' (positions 1338-1312). Inner primers were AS31 (+): 5'-GAAAAA-ATTAGGCTACGACCCGGCGGAAAG-3' (positions 1089-1118), and AS32 (-): 5'-TTATAAAGGCTTTTTAAATTTTCT-3' (positions 1279-1256). PCR reaction mixtures contained 10 mM Tris, pH 8.3, 50 mM KCl, 1.5 mM MgCl<sub>2</sub>, 2.5 U Taq DNA polymerase (Perkin-Elmer, Emeryville, CA) and 100 ng of each (+) and (-) primer. Cycling conditions were 30 cycles at 94°C for 15 s, 55°C for 1 min, and 72°C for 1 min 45 s, in a final volume of 100  $\mu$ l. A 5- $\mu$ l aliquot of the product from the outer primers was used in the inner PCR, and the resultant PCR product visualized as a 190-bp product by ethidium bromide staining after agarose gel electrophoresis. All blocks were tested at least twice in this manner. A random sampling of PCR products was sequenced using Sequenase 2.0 (United States Biochemical Corp.) to verify that the amplified fragment was, in fact, the SIV gag gene.

For in situ PCR, 8- $\mu$ m sections were cut onto a silanized slide with a clean, disposable microtome blade. The samples were deparaffinized in xylene and hydrated through graded alcohols and air dried. After rehydration in PBS, the samples were digested in proteinase K (20  $\mu$ g/ml) in lysis buffer (20 mM Tris, pH 8.0, 0.5% SDS) for 45 min to 1 h at 37°C, and the slide was then heated to 95°C for 1 min to inactivate the proteinase K. The slides were washed in PBS for 1 min, dehydrated through graded alcohols, and air dried before placement on a slidecycler (Coy Laboratories, Detroit, MI) preheated to 82°C. Each slide was rehydrated in 40  $\mu$ l of a PCR reaction mixture consisting of 10 mM Tris, pH 8.3, 1.5 mM MgCl<sub>2</sub>, 0.25 mM dATP, 0.25 mM dCTP, 0.25 mM dGTP, 0.14 mM dTTP, 12.9  $\mu$ M digoxigenin-11-dUTP (Boehringer Mannheim Corp., Indianapolis, IN), and 50 ng of each primer (AS29 and AS30), preheated to 94°C for 1 min. Subsequently, 0.75  $\mu$ l (5 U/ $\mu$ l) Taq DNA polymerase was added to initiate the hot-start PCR reaction. The samples were covered with a 22  $\times$  40-mm glass coverslip, sealed with nail polish, and cycled for 25 cycles of 94°C for 1 min, 56°C for 2 min, and 72°C for 2 min.

After cycling, the coverslip was removed, and the slides were washed twice for 5 min in PBS. A 1:1,000 dilution of alkaline phosphatase-conjugated antidigoxigenin (Boehringer Mannheim Corp.) in PBS was added to the slides, which were then incubated overnight at 4°C. The slides were washed twice with PBS, and then incubated for 30 min with nitroblue tetrazolium (NBT; 337.5  $\mu$ g/ml) and 5-bromo-4-chloro-3-indolyl phosphate (BCIP; 175  $\mu$ g/ml) in alkaline phosphatase buffer (100 mM Tris, 100

mM NaCl, 50 mM MgCl<sub>2</sub>, pH 9.5) for 15-30 min at ambient temperature in the dark. Slides were then washed in water, counterstained with fast green, washed again, and mounted using Crystal/Mount (Biomedex, Culver City, CA). Positive cells yielded a black nuclear precipitate.

Controls for the in situ PCR assay included tissue from Rh Co and Rh HI, tissue from paraffin blocks that were negative by solution-phase PCR, and serial sections of slides with positive signal to which no Taq DNA polymerase or primer was added, or the use of the HIV-1 primers SK38/SK39 (28) in place of SIV primers. More than 40 control slides were tested in parallel under these conditions, and positive cells were never detected in any sections. Sections in which SIV<sup>+</sup> cells were found were confirmed as positive by studying more than five sections.

**Immunohistochemistry.** Immunohistochemistry was performed using the LSAB, LSAB2, and Doublestain kits (Dako Diagnostics) according to the manufacturer's instructions. Sections were deparaffinized and rehydrated through graded alcohols and Tris-buffered saline as above. The following antibodies (all from Dako Diagnostics) and dilutions were used, which were found to cross-react with macaque antigens: MHC class II, mouse anti-human HLA-DR (clone TAL.1B5), 1:50; mouse anti-human HLA-DR, DP, DQ, DX (clone CR3/43), 1:50; monocyte/macrophages, mouse anti-human CD68 (clones KP1 and PG-M1), 1:50; T lymphocytes, rabbit anti-human CD3 (polyclonal), 1:25; and dendritic cells, rabbit anti-cow S-100 (polyclonal), 1:100. The following dendritic cell antibodies were tested but failed to react with fixed-embedded macaque tissue: mouse anti-human CD1a (clone 010; Immunotech, Westbrook, ME), mouse anti-human B70/B7-2 (clone IT209; courtesy of Ed Engleman, Stanford University, Stanford, CA) (29), and mouse anti-human F-actin (clone 55K2; AIDS Research and Reference Reagent Program, NIAID, NIH) (30). When applicable, slides were counterstained with Mayer's hematoxylin and mounted as described above. Controls for antibody staining included identically processed macaque spleen and lymph nodes. Hematoxylin and eosin staining of slides was performed per standard protocols (31).

## Results

*The First Cellular Targets of SIV Infection Are Found in the Lamina Propria, Immediately Adjacent to the Epithelium.* To determine the first cellular target of SIV infection in the mucosa, we inoculated four female rhesus macaques intravaginally and atraumatically with a 70% animal infectious dose of SIVmac251 (23, 42, 43), and killed the animals 2, 5, 7, and 9 d later (designated Rh D2, Rh D5, Rh D7, and Rh D9, respectively). An animal inoculated with heat-inactivated SIVmac251 (Rh HI) in an identical manner and killed 2 d later, and an uninoculated animal (Rh Co) were used as controls. At necropsy, the vagina, cervix, spleen, and lymph nodes were harvested, fixed, and embedded in paraffin blocks. To screen for the presence of SIV provirus in the embedded tissue samples, cellular DNA was extracted and tested using a nested PCR for SIV gag. In this manner, we determined that vaginal tissues from all four inoculated animals contained provirus, whereas tissues from both control animals did not.

To identify the infected cells in the cervicovaginal mucosa, we subjected those tissue blocks found to contain SIV gag sequences by nested PCR to in situ PCR in the pres-

ence of digoxigenin-dUTP and determined which cells contained amplified product using an antibody directed against digoxigenin (32, 33). Representative results are presented in Fig. 1. Low-power magnification of the stratified squamous epithelium and the adjacent lamina propria from Rh D2 and Rh D5 are shown in Fig. 1, A and B, respectively. We found many SIV-infected cells in the lamina propria immediately subjacent to the epithelium, but none within the epithelium. Similarly, SIV-infected cells were only found immediately beneath the simple columnar epithelium of the endocervix of Rh D5 (Fig. 1 C). An identical pattern of infection was demonstrable in all four experimental animals. Higher magnification examination of the vaginal (Fig. 1, D–F) and the endocervical (Fig. 1, G–I) mucosa confirmed the nested PCR results that SIV-infected cells were present in all four experimental animals. In each monkey, SIV-infected cells were abundant in the lamina propria, but were absent in the overlying epithelium. Most SIV-infected cells were usually only a small distance (<25  $\mu\text{m}$ ) away from the basement membrane,

which separates the epithelium from the lamina propria. As the distance from the epithelial border increased, the number of SIV-infected cells decreased dramatically. Occasional positive cells were also found deeper (not shown), on the order of hundreds of microns to as much as 1 cm away from the epithelial border.

To control for the specificity in detecting in situ PCR-amplified SIV gag DNA, numerous controls were tested in parallel, and the results are shown in Fig. 2. These included tissues from control animals (Rh Co and Rh HI; Fig. 2, A and B) and a block of tissue from Rh D5 that was found not to contain SIV by nested PCR (Fig. 2 C). Nonspecific alkaline phosphatase staining was not observed (not shown).

*Morphology and Immunohistochemistry Suggest that SIV-infected Cells Are Likely to be Dendritic Cells.* Upon close examination, it became apparent that SIV-infected cells were morphologically diverse (Fig. 1). Although many cells were small and round, typical of lymphocytes, many were not. A sampling of the latter is shown under higher magnification in Fig. 3. Their size and morphology suggest that many

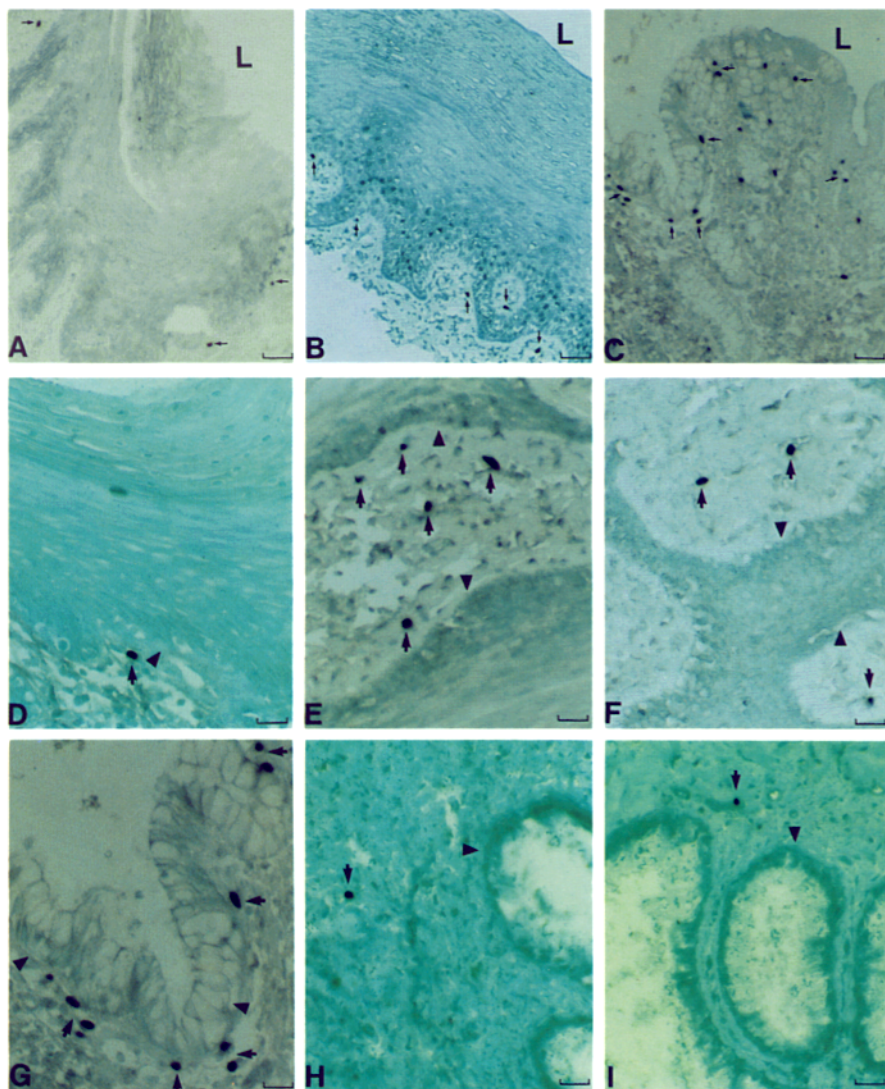


**Figure 1.** Detection of SIV-infected cells in the mucosa of inoculated animals. Low magnification: (A) Rh D2, vagina; (B) Rh D5, vagina; (C) Rh D5, endocervix. Higher magnification, vagina: (D) Rh D2; (E) Rh D7; (F) Rh D9. Higher magnification, endocervix: (G) Rh D5; (H) Rh D7; (I) Rh D9. Positive cells detected after in situ PCR are indicated with  $\uparrow$ , the basement membrane with  $\blacktriangle$ , and the vaginal lumen with L. Note location of infected cells in lamina propria, immediately adjacent to the epithelium, but lack of positive cells in the epithelium itself. In situ PCR was carried out in the presence of digoxigenin-dUTP, followed by incubation with alkaline phosphatase-conjugated antidigoxigenin and NBT/BCIP (see Materials and Methods). The nuclei of positive cells stain black. The sections were counterstained with fast green and viewed under light microscopy. Bars: (A–C) 100  $\mu\text{m}$ ; (D–I) 50  $\mu\text{m}$ .

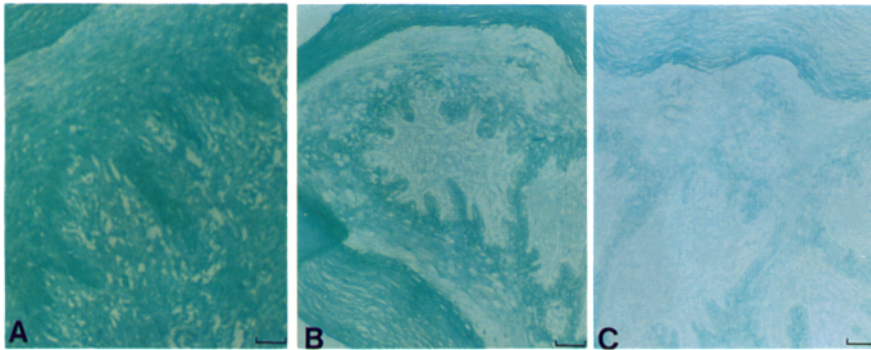


**Figure 2.** Controls for detection of in situ PCR-amplified product. Typical sections showing lack of infected cells from: (A) Rh HI, (B) Rh Co, (C) Rh D5, tissue section negative by nested PCR. Sections were counterstained with fast green and viewed under light microscopy. Of >40 controls run in parallel with samples (see Fig. 1), positive cells were never detected. Bars, 100  $\mu\text{m}$ .

cells were not small lymphocytes, like those found in blood. Because APC such as dendritic cells and macrophages express CD4, and because of the potential role of dendritic cells in establishing a local, productive site for HIV-1 replication (16, 34), we surmised that many of these larger non-lymphocytic cells might be Langerhans dendritic cells. Although cellular morphology was maintained, the extensive heat treatment and proteinase K digestion necessary for PCR destroyed the antigenic markers of the cells we were interested in studying. Therefore, we relied on studies of serial, contiguous (8- $\mu\text{m}$ ) sections.

With this in mind, we identified infected cells after in situ PCR as above in conjunction with performing immunohistochemistry on a contiguous section. For example, Fig. 4 A shows SIV-infected cells detected by in situ PCR in the vaginal lamina propria of Rh D5, and Fig. 4 B depicts an adjacent section stained for MHC class II molecules. In this tissue, MHC class II is expressed in high levels on APC and B cells, whereas activated T cells express only very low levels of this antigen. SIV-infected cells in many other tissue sections correlated with MHC class II staining on contiguous sections and had long processes characteristic of APC. To specifically identify dendritic cells, we stained for the S-100 antigen, which in mucosal tissue is found on dendritic cells and cells of neural crest origin. As another example, Fig. 4 C shows an SIV-infected cell detected after in situ PCR, whereas Fig. 4 D shows an S-100<sup>+</sup> cell with long processes in the same location on the adjacent section. Using this type of analysis, we were unable to detect macrophages (cells expressing the CD68 antigen) that were contiguous to SIV infected cells (data not shown). Although our studies are obviously not conclusive, there is evidence to suggest that nonlymphocytic cells are targets of SIV infection in acute infection.

*Evidence for Focal Viral Spread and Syncytia Formation in Deeper Mucosal Dendritic Cells.* In addition to positive cells found near the epithelium, we found occasional SIV-infected cells in the deeper tissue from each of the animals. An extreme example of this in Rh D2 is shown in Fig. 5 A, representing an area containing a nerve ganglion distant from the epithelium. The neurons, as expected, were not infected with SIV. However, many cells surrounding the neurons were infected, and among these cells, syncytia formation was evident. Many of the positive cells are large, with elongated nuclei, indicating that they are unlikely to be lymphocytes, but more likely to be APC (Fig. 5 A).

To test this assumption, we stained contiguous sections for MHC class II (Fig. 5, B and C), CD3 (T cells; Fig. 5 C), and CD68 (macrophages; Fig. 5 D). Many of the cells, having processes characteristic of APC, clearly expressed MHC class II antigens. There was virtually no staining for macrophages (Fig. 5 D), however, and only a few cells stained for CD3 (Fig. 5 C). The morphology, staining for MHC class II, and lack of staining with anti-CD68 demonstrate that most of these are likely to be dendritic cells or dendritic cell-T cell syncytia. These cells, therefore, are clearly capable of forming syncytia and spreading SIV to deeper mucosal tissues only a short time (2 d) after an intravaginal inoculation.

*Viral Dissemination Occurs through the Draining Lymphatics.* To determine the route and time course of viral dissemination from the mucosa, we obtained the draining and peripheral lymph nodes from the animals at necropsy. In both humans and macaques, the lymphatic drainage of the area to which the inoculum was applied, the upper two thirds of the vagina, the cervix, and the uterus, is to the internal iliac lymph nodes, which are located along the internal iliac blood vessels, deep within the pelvis (35). To monitor the

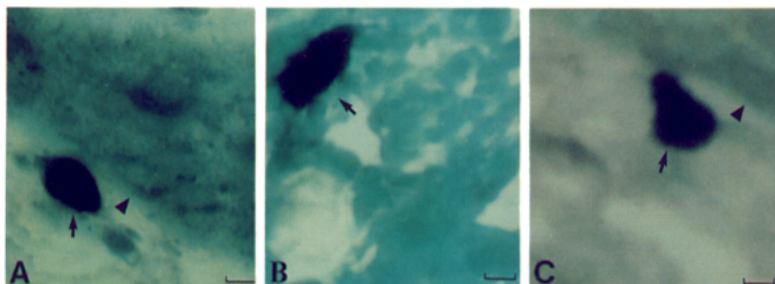


**Figure 3.** High-power magnification of SIV-infected cells demonstrating nonlymphocytic morphology. Note elongated, irregular shaped, large cells ( $\uparrow$ ) and their proximity to the basement membrane ( $\blacktriangle$ ). Fast green counterstain. Tissue sections are from Rh D5 and Rh D7. Bars, 12.5  $\mu\text{m}$ .

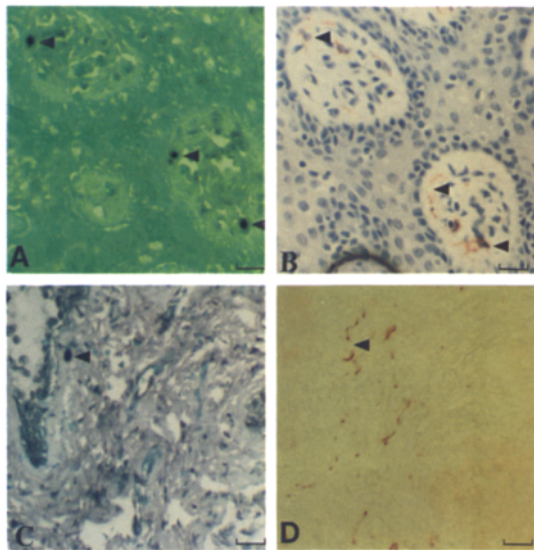


**Figure 4.** Serial section studies: SIV-infected cells correlate with the location of APC and dendritic cells in the mucosa. Correlation of SIV-infected cells detected after in situ PCR with immunohistochemistry performed on the contiguous (8- $\mu$ m) section. Cells infected with SIV and their corresponding cells in contiguous sections are labeled with  $\blacktriangle$ . Tissue sections are from Rh D5. (A and C) In situ PCR for SIV, fast green counterstain. Immunocytochemistry: (B) MHC class II, section adjacent to A, hematoxylin counterstain. (D) S-100, section adjacent to B, no counterstain. Cells expressing antigen are stained red with peroxidase/3-amino-9-ethylcarbazole (AEC). Bars, 50  $\mu$ m.

periphery for viral spread, we also obtained “nondraining” lymph nodes from the axillary and inguinal regions, as well as PBMC, splenic lymphocytes, and plasma. These samples were analyzed for the presence of SIV by culture (Table 1)

and PCR (Table 2). Of all the samples tested, the only ones from which we were able to isolate virus by culture were from Rh D5. In this animal, terminal-bleed PBMC and the internal iliac lymph nodes (three of four tested) contained infectious virus. None of the peripheral nodes from this animal were positive by culture (Table 1).

PCR, however, demonstrated the presence of provirus throughout the lymphatic tissues of all four experimental animals (Table 2); control animals (Rh HI and Rh Co) were consistently negative. As early as 2 d after infection (Rh D2), the draining (internal iliac) lymph nodes contained provirus. The appearance of virus in the peripheral lymph nodes, however, was infrequent at day 2. In Rh D2, only one of six peripheral lymph nodes tested contained provirus, whereas in Rh D5 and all later animals, many of the peripheral lymph nodes were positive for provirus. From these results, we conclude that, within 2 d of a mucosal inoculation, infected cells quickly disseminate virus to the draining lymph nodes. Once there, systemic dissemination occurs shortly thereafter.

*The Internal Iliac Lymph Nodes Demonstrate a Low Level of Infected Cells in the T Cell–dependent Regions and the Subcapsular Sinus.* Because of the above observations, we were interested in determining the frequency and location of infected cells in the internal iliac lymph nodes. To do this, we detected SIV-infected cells by in situ PCR in lymph nodes from Rh D5, which were found to contain SIV by both culture and nested PCR. Fig. 6 A shows SIV-infected cells from one such lymph node, and hematoxylin and eosin staining of an adjacent section (Fig. 6 B) demonstrates that these cells localize to the subcapsular sinus of the lymph node. Infected cells were also localized to the T

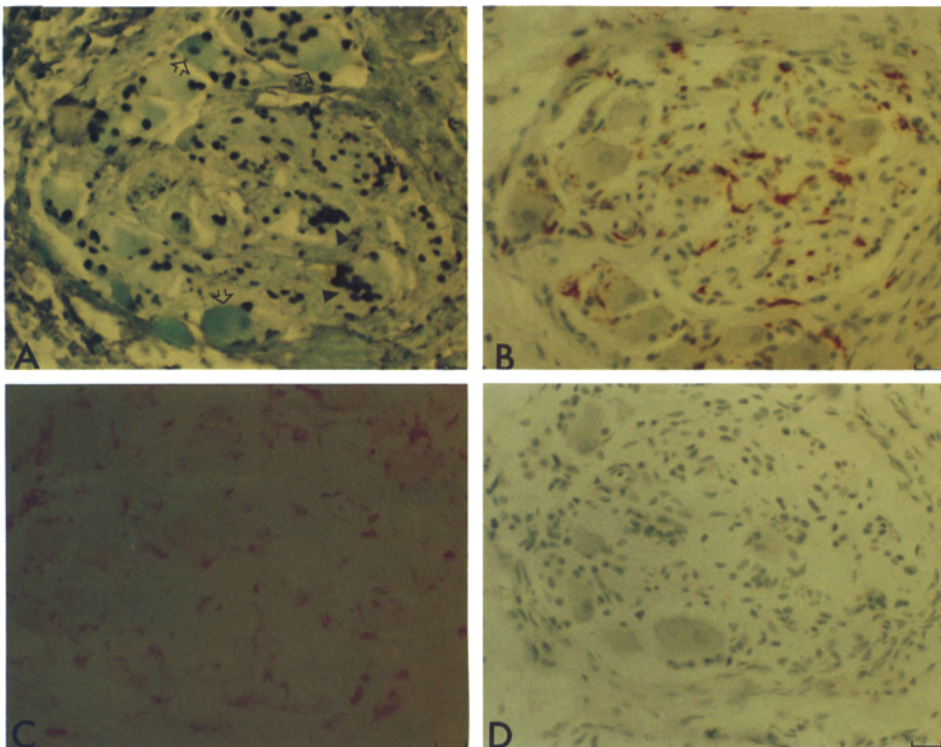


**Figure 5.** Evidence for the spread of infection in deep mucosal dendritic cells by 2 d after vaginal inoculation (Rh D2). (A) In situ PCR. Region shown is a nerve ganglion surrounded with SIV-infected cells. Note uninfected neuron ( $\cap$ ) and formation of syncytia ( $\blacktriangle$ ). Immunocytochemistry on serial (8- $\mu$ m) sections: (B) MHC class II (red), peroxidase/AEC staining, hematoxylin counterstain. (C) CD3 (brown) and MHC class II (pink). MHC class II, alkaline phosphatase–antialkaline phosphatase/fast red staining; CD3, peroxidase/diaminobenzidine staining, not counterstained. (D) CD68 (red), stained as in B. This area contains numerous MHC class II–expressing cells, but virtually no macrophages or T cells, demonstrating that a majority of the infected cells in this area are dendritic cells. Bars, 50  $\mu$ m.

**Table 1.** Ability to Isolate SIV by Culture

Sample	Rh D2	Rh D5	Rh D7	Rh D9	Rh HI
PBMC					
Day 2	—	—	—	—	—
Day 5		+	—	—	
Day 7			—	—	
Day 9				—	
Plasma					
Day 2	—	—	—	—	—
Day 5		—	—	—	
Day 7			—	—	
Day 9				—	
Spleen	—	—	—	—	—
Lymph Nodes					
Axillary	—	—	—	—	—
Inguinal	—	—	—	—	—
Paraortic		—	—	—	—
Iliac	—	+ (3/4)*	—	—	—

\*Three of four samples were positive; the negative sample was the most superior along the internal iliac artery.

cell-dependent, paracortical zone of the draining lymph node (Fig. 6, C and D). In no case were infected cells found in the germinal centers. A picture emerges to suggest that SIV-infected cells migrate to the draining lymph node via the afferent lymphatics and enter the node through the subcapsular sinus. From here, these cells traverse to the T cell-dependent areas in the paracortical regions of the nodes. This pathway of migration is similar to that described for the movement of tissue dendritic cells (36).

## Discussion

In our model of a cell-free vaginal transmission, the first SIV-infected cell was found in the lamina propria, and not

in the epithelium. As shown in Fig. 1, these cells are usually in immediate proximity to the basement membrane of the epithelium and are found in high numbers in both the stratified squamous vagina/ectocervix and the simple columnar endocervix. It has been hypothesized by others (2, 15, 19, 37) that based on the known location of CD4<sup>+</sup> cells in the vaginal tract, the first cell to be infected would be an intraepithelial Langerhans cell. In these studies, however, we could find no evidence of infection in the epithelium itself. Studies in chronically infected animals have shown a much broader, including intraepithelial, presence of SIV-infected cells (19, 20), thereby countering arguments that the infected cells we find are the result of secondary viral replication.

This multilayered epithelium may act as a physical barrier to repel most of the invading virus, and it is only those few viral particles that are able to penetrate into the lamina propria that can initiate an infection. How does the virus make it through the epithelial barrier? The stratified epithelium of the vagina is not the tight, impenetrable barrier of the skin. Although aglandular, it is moist, and fluid is continuously passing through the intercellular space from the lamina propria. Epithelial cells are connected by discontinuous patches of desmosomes, the weakest form of intercellular junction. This, at best, keeps the cellular membranes 30 nm apart (38). Although still significantly smaller than a retroviral particle (100–150 nm), it is possible that a small fraction of the viruses in the inoculum may be able to permeate through the entire epithelium to the lamina propria. Another possibility is that the virus may bind to Langerhans cells in the epithelium without infecting them, as has been shown to happen in the case of blood-derived dendritic cells (16). These virus-bound cells, which would not be detected by our *in situ* PCR to detect SIV DNA, could then migrate to the lamina propria and there infect the first CD4-positive cell encountered. Although not observed macroscopically or microscopically, there may be some disruption in the integrity of the epithelium at the time of inoculation, which would permit passage of some virus to the lamina propria. Lastly, though not present in the vagina, M cells in the intestine have been shown to

**Table 2.** Ability to Detect SIV by PCR

Sample	Rh D2	Rh D5	Rh D7	Rh D9	Rh HI	Rh Co
PBMC						
Day 2	—	—	—	—	—	
Day 5		—	—	—		
Day 7			—	—		
Day 9				—		
Spleen	+	+	+	+	—	—
Lymph Nodes						
Internal iliac	+ (3/4)	+ (4/7)	+ (1/1)	+ (3/5)	—	—
Axillary	+ (1/2)	+ (3/7)	+ (2/4)	+ (4/8)	—	—
Inguinal	— (0/4)	+ (2/6)	+ (2/3)	+ (2/3)	—	—

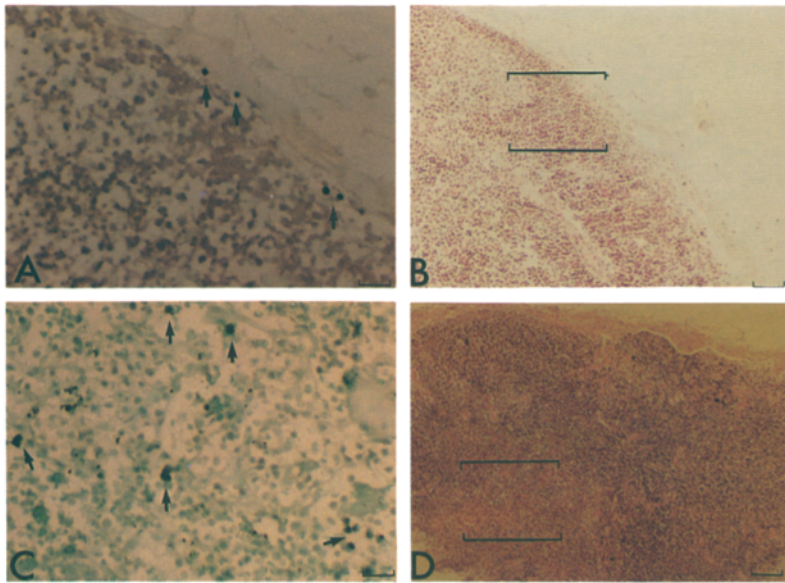


**Figure 6.** Localization of infected cells in the draining lymph nodes in R.h D5. Cells infected with SIV are labeled with  $\uparrow$ . (A) In situ PCR, fast green counterstain. This section represents the subcapsular sinus of the lymph node delineated by the brackets shown in B; hematoxylin and eosin stain. (C) In situ PCR. This section represents the T cell-dependent region (paracortical zone) of the lymph node delineated by the brackets shown in D; hematoxylin and eosin stain. Controls identical to those in Fig. 2 were run in parallel. Dark spots not labelled are hemoglobin debris from necropsy. Bars: (A and C) 100  $\mu\text{m}$ ; (B and D) 250  $\mu\text{m}$ .

carry virus across the epithelium (39), so a similar, as yet undefined mechanism may be operative in the vaginal mucosa. Despite these possibilities, we cannot yet definitively determine how SIV crossed the epithelium.

It is possible that for transmission to occur, transport of virus across the epithelium (columnar or squamous) to the lamina propria is indeed a limiting factor in infection efficiency. Viruses such as poliovirus, herpesvirus, and rhinovirus have been shown to directly infect epithelial cells (40), which may explain why these viruses are more easily transmitted than HIV. It might be expected that passage through a single layer of epithelial cells to the lamina propria—as in the endocervix (Fig. 2)—is far easier than passage through multiple layers. Histologically, the rectum is similar to the endocervix, with a simple columnar epithelium. Based on our observations, we hypothesize that at least some of the increased risk of HIV-1 transmission associated with anal intercourse is due to this thinner epithelium. Although the endocervical epithelium is simple columnar, physical barriers such as the high levels of mucous present at the external os, combined with its limited accessibility and relatively small surface area, may greatly reduce the exposure of this tissue to virus.

As described previously (3, 7), sexual transmission of HIV-1 appears to be selective in that certain minor viral variants from the infecting mixtures of viruses are preferentially transmitted. We now provide evidence that cells in the lamina propria of the cervicovaginal mucosa that resemble dendritic cells may play a role in the selection mechanism. Because of the known diversity of HIV-1 functional phenotypes, it may be that certain viral variants infect the mucosal dendritic cell with greater efficiency, leading to establishment of infection by those variants. This underscores the importance of developing vaccines against primary HIV-1 isolates found in recently infected persons rather than against laboratory strains.

Trafficking of lymphocytes and APC has been well de-

fined. From mucosal sites, primarily APC but also lymphocytes migrate into the afferent lymphatics. From there, they enter the lymph nodes through the subcapsular sinus and traverse toward the T cell areas in the paracortical regions. Whereas APC terminate here, lymphocytes can leave through the efferent lymphatics, enter the thoracic duct, and spread hematogenously. This is precisely the same migration pattern we have observed for SIV spread, which is schematically summarized in Fig. 7. The first targets of in-

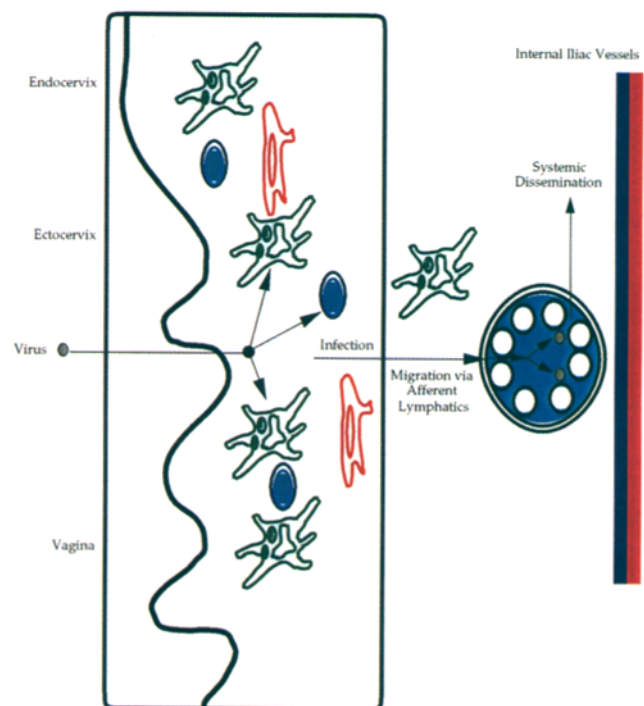


**Figure 7.** Model for mucosal transmission of SIV and HIV. See text for the discussion. Dendritic cells are shown in green, macrophages in red, lymphocytes in blue, and virus in grey.

fection were found in the lamina propria, and we also observed local spread within the mucosa itself. Within 2 d of inoculation, infected cells have migrated to the draining lymph nodes, which appear to be a major site of viral replication. After deposition and replication of virus in the T cell-dependent regions of the lymph nodes (Fig. 6), infected T cells and free virus can leave through the efferent lymphatics and disseminate widely. We can only speculate that sexual transmission of HIV-1 follows a similar pathway.

It is significant that despite the presence of CD4<sup>+</sup> cells in the epithelium (19, 20), we were unable to detect infected cells there. It has been reported that the best milieu for infection by HIV-1 in vitro is conjugates of lymphocytes and dendritic cells (34). In uninfected animals, we have found many more dendritic cells in the lamina propria than in the epithelium itself, and it is possible that the former is the optimal milieu for efficient infection. An infected dendritic cell can present the virus to many T cells in the mucosa or after trafficking to the lymph nodes, resulting in substantial amplification of the virus. In the lamina propria of the colonic mucosa, it is also the dendritic cell that is the major APC, and the primary means by which T cells are activated (41). It might be expected that any factor that results in increased antigen presentation at the time of transmission, such as a concomitant infection, could result in more efficient viral spread. Although our studies cannot definitively identify the infected cell population, the cells that are SIV-infected are in regions (Figs. 4 and 5) that contain large numbers of MHC class II<sup>+</sup> and S-100<sup>+</sup> cells, and are thus likely to be dendritic cells.

Whereas in previous studies a single dose of the inoculum we used has led to culturable viremia in only 70% of animals inoculated intravaginally (42, 43), 100% of the four experimental animals in this study demonstrated infected cells at the site of inoculation, in the draining lymph nodes, and in the peripheral lymphoid tissue. Because these animals were killed early, aside from Rh D5, it is impossible to say which animals would have developed an obvious disseminated infection (Table 1). Studies to determine if a limited mucosal infection can occur without systemic dissemination are underway. This may also be relevant to the phenomenon of transient infections, previously noted in macaques inoculated intravaginally (44).

Our findings on the mucosal transmission of SIV have important implications for vaccine development. A vaccine must induce immune responses that effectively block at least one of the steps in the earliest stages of infection. One way to protect is via mucosal antibodies that neutralize virus before it infects its initial target cell in the lamina propria. In addition, throughout the vaginal mucosa of normal animals lie a large number of CD8<sup>+</sup> lymphocytes (2, 20), which could destroy cells that become productively infected with virus. Furthermore, because of the importance of the draining lymphatics in viral dissemination, it might be expected that a specific antiviral immune response here would be extremely effective in preventing the establishment of infection. In future studies, it would be interesting to examine the steps in SIV transmission and spread that are blocked by an efficacious vaccine, such as the live attenuated virus (45).

---

We are grateful to A. Gettie and C. Russo for technical assistance, Dr. J. Vanderburg for the use of microtome, R. Steinman and M. Pope for helpful advice, J. Moore for critical comments on the manuscript, and W. Chen for preparation of the figures.

This work was supported by National Institutes of Health (NIH) grants AI-24030, AI-25541, AI-35522, AI-32427, AI-27665, AI-28147, and HD-31756, the New York University Center for AIDS Research (AI-27742), and the Aaron Diamond Foundation. A. I. Spira was supported by an NIH Medical Scientist Training Program Fellowship (GM-07038), a Merck Corporation Scholarship, and a grant from the Pediatric AIDS Foundation.

Address correspondence to David D. Ho, Aaron Diamond AIDS Research Center, New York University School of Medicine, 455 First Avenue, New York, NY 10016.

*Received for publication 13 July 1995 and in revised form 18 September 1995.*

## References

1. Padian, N., S. Shibosky, and N. Jewell. 1991. Female to male transmission of human immunodeficiency virus. *JAMA*. 266: 1664-1667.
2. Miller, C., J. McGhee, and M. Gardner. 1992. Mucosal immunity, HIV transmission, and AIDS. *Lab. Invest.* 68:129-145.
3. Zhu, T., H. Mo, N. Wang, D.S. Nam, Y. Cao, R.A. Koup, and D.D. Ho. 1993. Genotypic and phenotypic characterization of HIV-1 in patients with primary infection. *Science (Wash. DC)*. 261:1179-1181.
4. Wolinsky, S.M., C. Wike, B. Korber, C. Hutto, W. Parks, L. Rosenblum, K. Kunstman, M. Furtado, and J. Munoz. 1992. Selective transmission of human immunodeficiency virus type-1 variants from mothers to infants. *Science (Wash. DC)*. 255:1134-1137.
- 4a. Zhu, T., N. Wang, A. Carr, D.S. Nam, D.A. Cooper, and D.D. Ho. 1996. Genetic characterization of human immunodeficiency virus type 1 in blood and genital secretions: evidence for viral compartmentalization and selection during sexual transmission. *J. Virol.* In press.
5. Roos, M., J. Lange, R. DeGoede, R. Couthino, P. Schelekens, F. Miedema, and M. Tersmette. 1992. Viral phenotype

- and immune response in primary human immunodeficiency virus type 1 infection. *J. Infect. Dis.* 165:427-432.
6. Cornelissen, M., G. Mulder-Kampigna, J. Veenstra, F. Zorgdrager, C. Kuiiken, S. Hartman, J. Dekker, L. van der Hoek, C. Sol, R. Coutinho, and J. Goudsmit. 1995. Syncytium-inducing SI phenotype suppression at seroconversion after intramuscular inoculation of a non-syncytium inducing/SI phenotypically mixed human immunodeficiency virus population. *J. Virol.* 69:1810-1818.
  7. Zhang, L., P. Mackenzie, A. Cleland, E. Holmes, A. Leigh Brown, and P. Simmonds. 1993. Selection for specific sequences in the external envelope protein of human immunodeficiency virus type 1 upon primary infection. *J. Virol.* 67:3345-3356.
  8. Cann, A., M. Churcher, M. Boyd, W. O'Brien, J. Zhao, J. Zack, and I. Chen. 1992. The region of the envelope gene of human immunodeficiency virus type 1 responsible for determination of cell tropism. *J. Virol.* 66:305-309.
  9. Shioda, T., J. Levy, and C. Cheng-Mayer. 1991. Macrophage and T-cell line tropisms are determined by specific regions of the envelope gp120 gene. *Nature (Lond.)*. 349:167-169.
  10. Clark, S.J., M.S. Saag, W.D. Decker, S. Campbell-Hill, J.L. Roberson, P.J. Veldkamp, J.C. Kappes, B.H. Hahn, and G.M. Shaw. 1991. High titers of cytopathic virus in plasma of patients with symptomatic primary HIV-1 infection. *N. Engl. J. Med.* 324:954-960.
  11. Daar, E., T. Moudgil, R. Meyer, and D.D. Ho. 1991. Transient high levels of viremia in patients with primary human immunodeficiency virus type 1 infection. *N. Engl. J. Med.* 324:961-964.
  12. Koup, R.A., J.T. Safrit, Y. Cao, C. Andrews, G. McLeod, W. Borkowsky, C. Farthing, and D.D. Ho. 1994. Temporal association of cellular immune responses with the initial control of viremia in primary human immunodeficiency virus type 1 syndrome. *J. Virol.* 68:4659-4665.
  13. Wei, X., S.K. Ghosh, M.E. Taylor, V.A. Johnson, E. Emimi, P. Deutsch, J.D. Lifson, S. Bonhoeffer, M.A. Nowak, B. Hahn, et al. 1995. Viral dynamics in human immunodeficiency virus type 1 infection. *Nature (Lond.)*. 373:117-122.
  14. Ho, D.D., A.U. Neumann, A.S. Perelson, W. Chen, J. Leonard, and M.H. Markowitz. 1995. Rapid turnover of plasma virions and CD4 lymphocytes in HIV-1 infection. *Nature (Lond.)*. 373:123-126.
  15. Braathen, L., G. Ramirez, R. Hunze, and H. Gelderbloom. 1987. Langerhans cells as primary target cells for HIV infection. *Lancet* 2:1094.
  16. Cameron, P.U., P.S. Freudenthal, J.M. Barker, S. Gezelter, K. Inaba, and R.M. Steinman. 1992. Dendritic cells exposed to human immunodeficiency virus type-1 transmit a vigorous cytopathic infection to CD4<sup>+</sup> T-cells. *Science (Wash. DC)*. 257:383-387.
  17. Nuovo, G.J., A. Forde, P. MacConnell, and R. Fahrenwald. 1993. In situ detection of PCR-amplified HIV-1 nucleic acids and tumor necrosis factor cDNA in cervical tissues. *Am. J. Pathol.* 143:40-48.
  18. Miller, C.J., N.J. Alexander, S. Sutjipto, A.A. Lackner, A. Gettie, A.G. Hendrickx, L.J. Lowenstine, M. Jennings, and P.A. Marx. 1989. Genital mucosal transmission of simian immunodeficiency virus: animal model for heterosexual transmission of human immunodeficiency virus. *J. Virol.* 63:4277-4284.
  19. Miller, C.J., N.J. Alexander, P. Vogel, J. Anderson, and P.A. Marx. 1992. Mechanism of genital transmission of SIV: a hypothesis based on transmission studies and the location of SIV in the genital tract of chronically infected female rhesus macaques. *J. Med. Primatol.* 21:64-68.
  20. Miller, C.J., M. McChesney, and P.F. Moore. 1992. Langerhans cells, macrophages, and lymphocyte subsets in the cervix and vagina of rhesus macaques. *Lab. Invest.* 67:628-634.
  21. Desrosiers, R.C. 1990. The simian immunodeficiency viruses. *Annu. Rev. Immunol.* 8:557-578.
  22. Letvin, N.L., M.D. Daniel, P.K. Sehgal, R.C. Desrosiers, R.D. Hunt, L.M. Waldron, D.K. MacKoy, D.K. Schmidt, L.V. Chalifoux, and N.W. King. 1985. Induction of AIDS-like disease in macaque monkeys with T-cell tropic retrovirus STLV-III. *Science (Wash. DC)*. 230:71-73.
  23. Daniel, M.D., N.L. Letvin, N.W. King, M. Kannagi, P.K. Sehgal, R.D. Hunt, P.J. Kanki, M. Essex, and R.C. Desrosiers. 1985. Isolation of T-cell tropic virus HTLV-III like retrovirus from macaques. *Science (Wash. DC)*. 228:1201-1204.
  24. Dulbecco, R. 1988. End-point method measurement of the infectious titer of a viral sample. In *Virology*, 2nd ed. R. Dulbecco and H. Ginsberg, editors. J. B. Lippincott, Philadelphia, PA. 22-25.
  25. Lohman, B., J. Higgins, M. Marthas, P.A. Marx, and N. Pederson. 1991. Development of simian immunodeficiency virus isolation, titration, and neutralization assays which use whole blood from rhesus monkeys and an antigen capture enzyme-linked immunosorbent assay. *J. Clin. Microbiol.* 29:2187-2192.
  26. Hoxie, J., B. Haggarty, S. Bonser, J. Rackowski, H. Snah, and P. Kanki. 1988. Biological characterization of a simian immunodeficiency virus-like retrovirus HTLV-IV: evidence for CD4-associated molecules required for infection. *J. Virol.* 62:2557-2568.
  27. Moore, J.P., and Q.J. Sattentau. 1993. Detecting SIV gp120 and its interaction with soluble CD4 by ELISA. *AIDS Res. Hum. Retroviruses*. 9:1297-1299.
  28. Kellogg, D., and S. Kwok. 1990. Detection of human immunodeficiency virus. In *PCR Protocols*. M. Innis, D. Gelfand, J. Sninsky, and T. White, editors. Academic Press, San Diego, CA. 337-347.
  29. Fagnoni, F.F., M. Takamizawa, W.R. Godfrey, A. Rivas, M. Azuma, and K. Okumura, and E.G. Engleman. 1995. Role of B70/B7-2 in CD4<sup>+</sup> T-cell immune responses induced by dendritic cells. *Immunology*. 85:467-474.
  30. Yamashiro-Matsmura, S., and F. Matsumura. 1985. Purification and characterization of an F-actin-bundling 55-kilodalton protein from HeLa cells. *J. Biol. Chem.* 260:5087-5097.
  31. Clark, G. 1981. *Staining Procedures*, 4th ed. Williams and Wilkins, Baltimore, MD. 20-30.
  32. Patterson, B.K., M. Till, P. Otto, C. Goolsby, M.R. Furtado, L.J. McBride, and S.M. Wolinsky. 1993. Detection of HIV-1 DNA and messenger RNA in individual cells by PCR-driven in situ hybridization and flow cytometry. *Science (Wash. DC)*. 260:976-979.
  33. Korber, B.T.M., K.J. Kunstman, B.K. Patterson, M. Furtado, M.M. Mceville, R. Levy, and S.M. Wolinsky. 1994. Genetic differences between blood- and brain-derived viral sequences from human immunodeficiency virus type 1 infected patients: evidence of conserved elements in the V3 region of the envelope protein of brain-derived sequences. *J. Virol.* 68:7467-7481.
  34. Pope, M.J., M.G.H. Betjes, N. Romani, H. Hirmand, P.U. Cameron, L. Hoffmann, S. Gezelter, G. Schuler, and R.M. Steinman. 1994. Conjugates of dendritic cells and memory T

- lymphocytes from skin facilitate productive infection with HIV-1. *Cell*. 78:389–398.
35. Hartmann, C. 1933. *The Anatomy of the Rhesus Monkey*. Hafner Publishing, New York. 259–260.
  36. Roitt, I., J. Brostoff, and D. Male. 1989. *Immunology*. Gower Medical Publishing, London. 2.05–2.13.
  37. Niedecken, H., G. Lutz, R. Bauer, and H. Kreysel. 1987. Langerhans cells as primary target and vehicle for transmission of HIV. *Lancet* 2:519–520.
  38. Junquiera, L.C., J. Carniero, and R.O. Kelley. 1989. *Basic Histology*. 6th edition. Appleton and Lange, Norwalk, CT. 20–30.
  39. Amerongen, H., R. Weltzin, C. Farnet, P. Michetti, W. Hasektine, and M. Neutra. 1991. Transepithelial transport of HIV-1 by intestinal M-cells: a mechanism for transmission of AIDS. *J. Acquir. Immune Defic. Syndr.* 4:760–765.
  40. Tyler, K., and B. Fields. 1990. Pathogenesis of viral infections. In *Field's Virology*. 2nd edition. Raven Press, New York. 191–239.
  41. Pavli, P., D. Hume, E. Van de Pol, and W. Doe. 1993. Dendritic cells, the major antigen-presenting cells of the human colonic lamina propria. *Immunology*. 78:132–141.
  42. Marx, P.A., R. Compans, A. Gettie, J. Staas, R. Gilley, M. Mulligan, G. Yamschikov, D. Chen, and J. Eldridge. 1993. Protection against vaginal SIV transmission with a microencapsulated vaccine. *Science (Wash. DC)*. 260:1323–1327.
  43. Miller, C.J., N.J. Alexander, S. Sutjipto, S. Joye, A.G. Hendrickx, M. Jennings, and P.A. Marx. 1990. Effect of viral dose and nonoxynol-9 on the genital transmission of SIV in rhesus macaques. *J. Med. Primatol.* 19:401–409.
  44. Miller, C.J., M. Marthas, J. Torten, N.J. Alexander, J.P. Moore, G. Doncel, and A. Hendrickx. 1994. Intravaginal inoculation of rhesus macaques with cell free simian immunodeficiency virus results in persistent or transient viremia. *J. Virol.* 68:6391–6400.
  45. Daniel, M.D., F. Kirchhoff, S.C. Czajak, P.K. Sehgal, and R.C. Desrosiers. 1992. Protective effects of a live attenuated vaccine with a deletion in the nef gene. *Science (Wash. DC)*. 258:1938–1941.